Original Article

Silencing hsa_circ_0049271 attenuates hypoxia-reoxygenation (H/R)-induced myocardial cell injury via the miR-17-3p/FZD4 signaling axis

Huocheng Liao[1,2], Chun Xiao[2], Weiwei Li[2], Wenzhong Chen[2], Dingcheng Xiang[1,3]

[1]School of Clinical Medicine, Southern Medical University (PLA Southern Theater General Hospital), Guangzhou, China; [2]Cardiovascular Medicine, Huizhou Third People's Hospital, Huizhou, China; [3]Cardiovascular Medicine, General Hospital of Southern Theatre Command of PLA, Guangzhou, China

Contributions: (I) Conception and design: H Liao, D Xiang; (II) Administrative support: C Xiao; (III) Provision of study materials or patients: W Li; (IV) Collection and assembly of data: W Chen; (V) Data analysis and interpretation: D Xiang, H Liao; (VI) Manuscript writing: All authors; (VII) Final approval of manuscript: All authors.

Correspondence to: Dingcheng Xiang. Southern Medical University, Guangzhou, China. Email: dcxiang@foxmail.com.

Background: This study sought to explore the role and molecular mechanism of circ_0049271 in hypoxia-reoxygenation (H/R)-induced cardiomyocyte injury.

Methods: Significantly upregulated circular ribonucleic acids (circRNAs) in Gene Expression Omnibus (GEO) data sets were identified using a Venn diagram. A H9c2 (rat cardiomyocytes) cell model of acute myocardial infarction (AMI) was induced by 1% H/R. Quantitative reverse transcription-polymerase chain reaction was used to detect the expression levels of circ_0049271, miR-17-3p, and FZD4 in clinical blood samples and cells, and Cell Counting Kit-8 (CCK-8) was used to determine the proliferation rate of the cells in each group. Next, flow cytometry and Western blot were used to evaluate cell apoptosis. Biochemical tests and enzyme-linked immunosorbent assays (ELISAs) were then used to determine the activities/levels of the cell damage markers [i.e., creatine kinase (CK) and lactate dehydrogenase (LDH)], oxidative stress substances [i.e., malondialdehyde (MDA), reactive oxygen species (ROS), and superoxide dismutase (SOD)], and inflammatory factors [i.e., interleukin (IL)-1β, IL-6, and IL-8]. In addition, intermolecular interactions were verified using dual-luciferase reporter and RNA pull-down experiments.

Results: Circ_0049271 was significantly upregulated in both the blood of the AMI patients and the H/R-induced H9c2 cells. The knockdown of circ_0049271 increased the cell proliferation rate, decreased the apoptosis rate, inhibited oxidative stress (ROS and MDA were upregulated, and SOD was downregulated) and inflammatory responses (IL-1, IL-6, and IL-8 were downregulated), and relieved cell damage. However, the overexpression of circ_0049271 promoted H/R-induced H9c2 cell damage. Further experiments showed that miR-17-3p was a target of circ_0049271, and miR-17-3p was negatively correlated with circ_0049271 in the AMI blood samples. Additionally, miR-17-3p was found to target FZD4. A further exploration also revealed that miR-17-3p knockdown or FZD4 overexpression reversed the effects of si-circ_0049271 on the H/R-induced H9c2 cells; that is, miR-17-3p knockdown or FZD4 overexpression promoted H/R-induced injury in the H9c2 cells.

Conclusions: Circ_0049271 promoted cellular function damage (e.g., proliferation inhibition, apoptosis, oxidative stress, and inflammation) in H/R-induced H9c2 cardiomyocytes via the miR-17-3p/FZD4 signaling axis.

Keywords: Acute myocardial infarction (AMI); cardiomyocyte injury; circ_0049271; miR-17-3p; FZD4

Submitted Nov 21, 2022. Accepted for publication Jan 10, 2023. Published online Jan 31, 2023.
doi: 10.21037/atm-22-6331
View this article at: https://dx.doi.org/10.21037/atm-22-6331

Introduction

Acute myocardial infarction (AMI) is a heart-related disease with high morbidity and mortality, and the most serious cardiovascular disease in the world. In recent years, the incidence of AMI has increased year-by-year and has shown an increasing trend in younger individuals (1). With >790,000 AMI cases reported annually in the United States alone, AMI has become a prominent public health and social problem (1).

AMI is mainly caused by coronary occlusion, which not only results in the ischemic necrosis of cardiac tissue but also causes significant and irreversible damage to myocardial cells. The most prominent feature of AMI is myocardial damage caused by acute or persistent ischemia and hypoxia (2). Current clinical treatments for AMI include surgical interventions, interventional therapy, and thrombolysis. However, researchers have noted that these treatments can cause additional reperfusion injuries, such as myocardial cell death and microvascular system damage (3). There is accumulating evidence that myocardial infarction (MI) can lead to cardiac remodeling and further damage the heart (4). Inflammation and myocardial fibrosis are also key biological processes in cardiac remodeling after AMI (4). The inhibition of the cardiac inflammatory response has been shown to suppress infarction-induced cardiomyocyte apoptosis and inhibit myocardial fibrosis-mediated ventricular remodeling (5). Due to the insufficient regenerative capacity of the body's cardiomyocytes, it is important to develop effective alternatives to treat AMI and reduce cardiomyocyte loss.

Circular ribonucleic acid (circRNA) is an endogenous non-coding RNA characterized by a covalently closed cyclic structure. Due to its specific structure, circRNA has good stability, a long duration of action, and good resistance to RNA exonuclease (6). Additionally, circRNAs can adsorb micro RNAs (miRNAs) to regulate the expression of miRNAs and their downstream target genes. Through the above process, circRNAs perform extensive biological functions in various diseases, such as osteoporosis (7), cardiovascular diseases (8), nervous system diseases (9,10), and cancer (11). Thus, circRNAs have become a research hot spot in recent years, leading researchers to pay more attention to the important role of circRNAs in the pathophysiology of cardiovascular diseases. For example, Zhou *et al.* reported that circRNA ACR (Autophagy related cyclic) targets Pink1-mediated FAM65B phosphorylation to inhibit the autophagy and death of cardiomyocytes, thereby alleviating cardiomyocyte injury (12). Li *et al.* found that the knockdown of circRNA circ-BNIP3 reversed the effects of hypoxia on the viability and apoptosis on the H9c2 cells via the miR-27a-3p/BNIP3 pathway (13).

The above findings suggest that circRNAs might be the key targets of AMI-mediated cardiomyocyte injury. However, the current literature on AMI-related circRNAs is not comprehensive. In addition, circRNAs mainly function by adsorbing microRNAs. As endogenous small non-coding RNAs with a length of 19–25 nt, miRNAs can bind to the 3'-untranslated region of target genes to play a role in degrading messenger RNA (mRNA) and blocking mRNA translation (14). Several studies have shown that miRNAs are related to various diseases and injuries, including AMI (15) and spinal cord injury (16). For example, Yuan *et al.* discovered that an increase in miR-21 level significantly reduced the MI area caused by AMI and inhibited cardiomyocyte apoptosis (17). MiR-17-3p was shown to target Par4 (Protease activated receptor 4) to regulate cell survival, growth, apoptosis, and EMT (Epithelial mesenchymal transition) and inhibit mouse cardiac fibroblast senescence (18). MiRNAs also play an important role in the progression of AMI.

In this study, we first conducted a differential analysis to screen the highly expressed circRNAs in AMI, and total 6 potential circRNAs (hsa_circ_0037516, chr16:15794592-15794782+, chr3:16336362-1634509, hsa_circ_0049271, hsa_circ_0076767, and hsa_circ_0023461) were screened from GSE160717 and GSE169594 datasets. Ren et al found that circ_0023461 knockdown attenuated hypoxia-induced dysfunction in AC16 cells partly by targeting the miR-370-3p/PDE4D axis (19). There are no studies about the effect

Highlight box

Key findings

- Circ_0049271 promoted cellular function damage in hypoxia-reoxygenation–induced H9c2 cardiomyocytes via the miR-17-3p/FZD4 signaling axis.

What is known and what is new?

- The current literature on AMI-related circRNAs is not comprehensive. In addition, circRNAs mainly function by adsorbing microRNAs.
- We first conducted a differential analysis to screen the highly expressed circRNAs in AMI and identified circ_0049271, which was then used to further explore the cardiomyocyte function and mechanism.

What is the implication, and what should change now?

- Circ_0049271 may serve as a potential therapeutic target for AMI.

of chr16:15794592-15794782+, chr3:16336362-1634509 and hsa_circ_0076767 on AMI. The bioinformatics analyses have found that circ_0049271 is abnormally expressed and plays a biological role in lung cancer (20,21) and systemic lupus erythematosus (22). Meanwhile, circ_0049271 might be related to diabetic foot ulcer infectious inflammation (23). We speculate that circ_0049271 may play a role in inflammation in myocardial injury, so we chose circ_0049271 for further exploring the cardiomyocyte function and mechanism. Using Cell Counting Kit-8 (CCK-8) and apoptosis assays, the effects of circ_0049271 on the proliferation and apoptosis of AMI cells were evaluated. Further, the miRNAs and miRNA target genes interacting with circ_0049271 in the AMI and the molecular mechanism of action were also explored. We present the following article in accordance with the MDAR reporting checklist (available at https://atm.amegroups.com/article/view/10.21037/atm-22-6331/rc).

Methods

Clinical sample collection

Blood samples were collected from AMI patients diagnosed and treated at Huizhou Third People's Hospital from November 2021 to February 2022 and healthy (normal) volunteers during the same period. The study was conducted in accordance with the Declaration of Helsinki (as revised in 2013). All the research procedures were approved by the Research Ethics Committee of Huizhou Third People's Hospital (No. 2022-8). The blood samples were collected after the participants voluntarily signed the informed consent. Peripheral blood mononuclear cells (PBMCs) were immediately isolated from the blood samples using Ficoll density gradient centrifugation.

To be eligible for inclusion in this study, the patients had to meet the following inclusion criteria: (I) meet the World Health Organization's diagnostic criteria for AMI; (II) have a clinical and imaging diagnosis of AMI; and (III) have signs or clinical symptoms of AMI. Patients were excluded from the study if they met any of the following exclusion criteria: (I) had an onset time >24 h; (II) had severe liver and kidney failure, a malignant tumor, a primary disease of the nervous system, or a mental illness; and/or (III) were a lactating or pregnant female.

Cell culture and transfection

Rat cardiomyocytes H9c2, purchased from the National Collection of Authenticated Cell Cultures (Shanghai, China), were cultured in Dulbecco's modified eagle medium with 10% fetal bovine serum (FBS, Gibco, USA) and 1% penicillin-streptomycin (Gibco, USA). The medium was placed in an incubator at 37 ℃ with 5% carbon dioxide. The cells were divided into the normal group and the hypoxia-reoxygenation (H/R) group. In the normal group, the H9c2 cells were cultured normally. Then we established the H/R-induced H9c2 cell model according to a previous study (24). Briefly, the H9c2 cells were maintained in serum-free DMEM (dulbecco's modified eagle medium) without glucose and cultured in a hypoxic incubator which contained 1% O_2, 5% CO_2 and 94% N_2 for 24 h. Then the cells were reoxygenated (95% air/5% CO_2) in fresh DMEM with 10% FBS for 2 h.

GenePharma (China) designed and synthesized the circ_0049271 interference fragment (si-circ_0049271) and its control (si-NC, negative control siRNA), circ_0049271 overexpression plasmid (circ_0049271), and its no-load control (Vector), the miR-17-3p mimic and its control (NC mimic), and the miR-17-3p inhibition agent (miR-17-3p inhibitor) and its control (NC inhibitor). After culturing to a logarithmic growth phase, the H9c2 cells were digested, collected and diluted to 2×10^6 cells/mL. Subsequently, the cells were seeded in 6-well plates. When cell confluence reached about 70%, the above small RNAs or plasmids were transfected into the cells using Lipofectamine 2000 (Invitrogen, USA). After 48 h of culture, the cells were collected.

Bioinformatics analysis

AMI-related circRNA expression datasets (GSE169594 and GSE160717) were obtained from the Gene Expression Omnibus (GEO) database (https://www.ncbi.nlm.nih.gov/geo/) (*Table 1*). We performed a differential analysis of the circRNA expression data in the AMI and corresponding control samples in the GSE data sets using limma package. A (log fold change) >1 was used as the cut-off criterion to define DE-circRNAs. The intersection of the upregulated DE-circRNAs from the GSE169594 data set (191 DE-circRNAs) and GSE160717 data set (201 DE-circRNAs) was then analyzed and screened by Venny 2.1.0 (https://bioinfogp.cnb.csic.es/tools/venny/) (25).

Quantitative reverse transcription-polymerase chain reaction (qRT-PCR)

The cell nucleus RNA and cytoplasm RNA were separated

Table 1 The basic information of the GEO data sets (GSE169594 and GSE160717)

GEO accession	Samples	Experiment type	Platforms
GSE169594	MCS, 4. AMI, 4.	Non-coding RNA profiling by array	GPL21825
GSE160717	NC, 3. AMI, 3.	Non-coding RNA profiling by array	GPL21825

GEO, Gene Expression Omnibus; MCS, mild coronary stenosis; AMI, acute myocardial infarction; NC, normal control.

Table 2 qRT-PCR primers

RNA	Sequences (5' to 3')
Circ_0049271	F: AACTTCGCTGAGCAGATTGG
	R: GCATGGGGTTCCAGAAGATA
Mir-17-3p	F: GCTCTGAUGUUCACGGAAGUG
	R: GTGCAGGGTCCGAGGT
FZD4	F: TTCACACCGCTCATCCAGTACG
	R: ACGGGTTCACAGCGTCTCTTGA
GAPDH	F: GTCTCCTCTGACTTCAACAGCG
	R: ACCACCCTGTTGCTGTAGCCAA
U6	F: CTCGCTTCGGCAGCACAT
	R: TTTGCGTGTCATCCTTGCG

qRT-PCR, quantitative reverse transcription-polymerase chain reaction.

in accordance with the instructions of the Cytoplasmic and Nuclear RNA Purification Kit (Cat. 21000, Norgen Biotek, Canada). Briefly, the cells were lysed using Lysis Buffer J and then centrifuged to separate cell fractions (pellet: nuclear fraction; supernatant: cytoplasmic fraction).

The supernatant and pellet were mixed with Buffer SK and absolute ethyl alcohol, respectively. Then combined the two mixtures with the centrifuge columns. Washed the columns with Wash Solution A. Finally, eluted the nuclear RNA and cytoplasmic RNA from centrifuge columns using Elution Buffer E.

The Trizol reagent was used to extract the total RNA from the cells and PBMCs of the peripheral blood. The concentration and purity of the RNA were then detected using NanoDrop. Subsequently, complementary deoxyribonucleic acid was prepared in accordance with the PrimeScript RT kit's instructions (Takara, Japan). Finally, the expression levels of circ_0049271, miR-17-3p, and FZD4 were determined according to the fluorescence polymerase chain reaction (PCR) kit's instructions (Takara, Japan). U6 or glyceraldehyde-3-phosphate dehydrogenase (GAPDH) was used as the internal control, and the experiment was replicated 6 time. For the experimental data obtained by qRT-PCR, the $2^{-\Delta\Delta Ct}$ method was used to calculate the relative expression level of target gene. The sequences of the primer used for this step are shown in *Table 2*.

CCK-8

A CCK-8 kit (Beyotime, China) was used to measure the cell proliferation rate. Specifically, in accordance with the instructions of the CCK-8 kit, the cells were digested, collected, and seeded in a 96-well plate at 1×10^4 cells/well. After the cells adhered to the wall, different treatments were performed. After 0 and 24 h of treatment, the cells were assayed following the instructions of the CCK-8 kit. Then, 20 μL of CCK-8 reagent and the cells were incubated at 37 ℃ for 2–4 h, and the optical density (OD) was measured at 450 nm using an enzyme-labeled-instrument to calculate the cell proliferation rate. Additionally, 6 duplicate wells were set up in the experiment, and the experiment was repeated 3 times.

Flow cytometry

After being digested by trypsin, the H9c2 cells were collected in centrifuge tubes. Next, the cells were rinsed twice with pre-cooled sterile phosphate-buffered saline (PBS). Subsequently, the cell concentration was adjusted to 5×10^5 cells/mL, and the apoptosis was measured in accordance with the instructions of the Annexin V—Fluorescein Isothiocyanate (FITC) Apoptosis Detection Kit (Beyotime, China). Finally, apoptotic cells marked with positive FITC and positive/negative PI were detected by flow cytometry.

Biochemical tests

The culture supernatant of the cells was collected after centrifugation at 2,000 r/min for 10 min at 4 ℃. Next, the cells were digested with trypsin and collected into centrifuge tubes. The cells were then washed twice with pre-cooled sterile PBS to obtain the cell suspension, and then underwent homogenization. Subsequently, the cell

slurry was collected by centrifugation. Finally, the activities of creatine kinase (CK) and lactate dehydrogenase (LDH) in the culture supernatant and the level of malondialdehyde (MDA), reactive oxygen species (ROS), and superoxide dismutase (SOD) in the cells were detected in accordance with the instructions of the corresponding biochemical kit (Jiancheng, Nanjing).

Enzyme-linked immunosorbent assays (ELISAs)

The cell suspension was collected. The contents of IL-1β, IL-6, and IL-8 in the suspension were determined in accordance with the instructions of the ELISA kit (Shanghai Enzyme-linked Biotechnology Co., Ltd., China). Finally, microplate readers were used to measure the OD at 450 nm (OD450).

Western blot

Radio immunoprecipitation assay lysis buffer (RIPA) cell lysate (Solebo, China) was used to extract the total protein of the cells, and the concentration of the extracted protein was determined using a bicinchoninic acid kit. Next, 20 μg of the proteins were separated by sodium dodecyl sulfate-polyacrylamide gel electrophoresis. The proteins were then transferred onto polyvinylidene fluoride membranes, blocked in 5% non-fat dry milk for 1–3 h, and primary antibodies [Bax, Bcl-2 (B-cell lymphoma-2), c-caspase-3, and GAPDH, Cell Signal Tech, USA] were added for incubation overnight at 4 ℃. Subsequently, the membranes were washed 3 times with tris-buffered saline and incubated in the secondary antibody dilution buffer for 1 h at ambient temperature. After washing the membranes 3 more times, enhanced chemiluminescence reagent (Solebo, China) was dripped onto the membranes. Subsequently, the membranes were placed in a gel imaging system to conduct protein development and image collection. ImageJ software was used to analyze the gray level of the protein bands, and GAPDH was used as the internal control to calculate the relative protein expression.

Dual-luciferase reporter gene

CircMIR 1.0 software and Targetscan 7.0 (http://www.targetscan.org/vert_70/) were used to predict the binding sites of circ_000049271 and miR-17-3p and miR-17-3p and FZD4, respectively. The wild-type (WT) or mutant (MUT) fragment of circ_0049271 or FZD4 was constructed into the dual-luciferase reporter plasmids (GP-miRGLO) (GenePharma). After the confluence reached about 80%, the 293T cells were co-transfected with the luciferase reporter plasmids and miR-17-3p mimic or NC mimic. The luciferase activity was measured using a dual-luciferase reporter kit 48 h after transfection (Promega, USA).

RNA pull-down

Biotinylated miR-17-3p (miR-17-3p-bio) and biotinylated control miR-NC (miR-NC-bio) were constructed. Specifically, the cell extracts (2 μg) were incubated with biotinylated RNA (100 pmol) for 1 h, and agarose beads (Invitrogen) were added for another 1 h of incubation. RNA was extracted, and the expression level of FZD4 or circ_0049271 in the precipitated complex was further detected using qRT-PCR.

Statistical analysis

All the results are expressed as the mean ± standard deviation (SD). The SPSS v26.0 software was used to perform the 1-way analyses of variance for comparisons among multiple groups and the *t*-test analyses for comparisons between 2 groups. Pearson correlation was used to analyze the correlations of the expression of circ_0049271, miR-17-3p, and FZD4 in the clinical blood samples. A P value <0.05 was used as the criterion for determining significant statistical difference.

Results

Circ_0049271 was significantly upregulated in the blood and H/R-induced H9c2 cells of the AMI patients

A differential analysis was performed on the AMI-related circRNA expression GEO data sets of GSE169594 and GSE160717. Next, 191 and 201 DE-circRNAs were screened from the GSE169594 and GSE160717 data sets (see Tables S1,S2). The intersections of the significantly upregulated circRNAs in the GSE169594 and GSE160717 data sets were analyzed using a Venn diagram (*Figure 1A*). The results of the intersections identified 6 potential circRNAs (i.e., hsa_circ_0037516, chr16:15794592-15794782+, chr3:16336362-1634509, hsa_circ_0049271, hsa_circ_0076767, and hsa_circ_0023461), from which, circ_0049271 was selected for the further cell experiments.

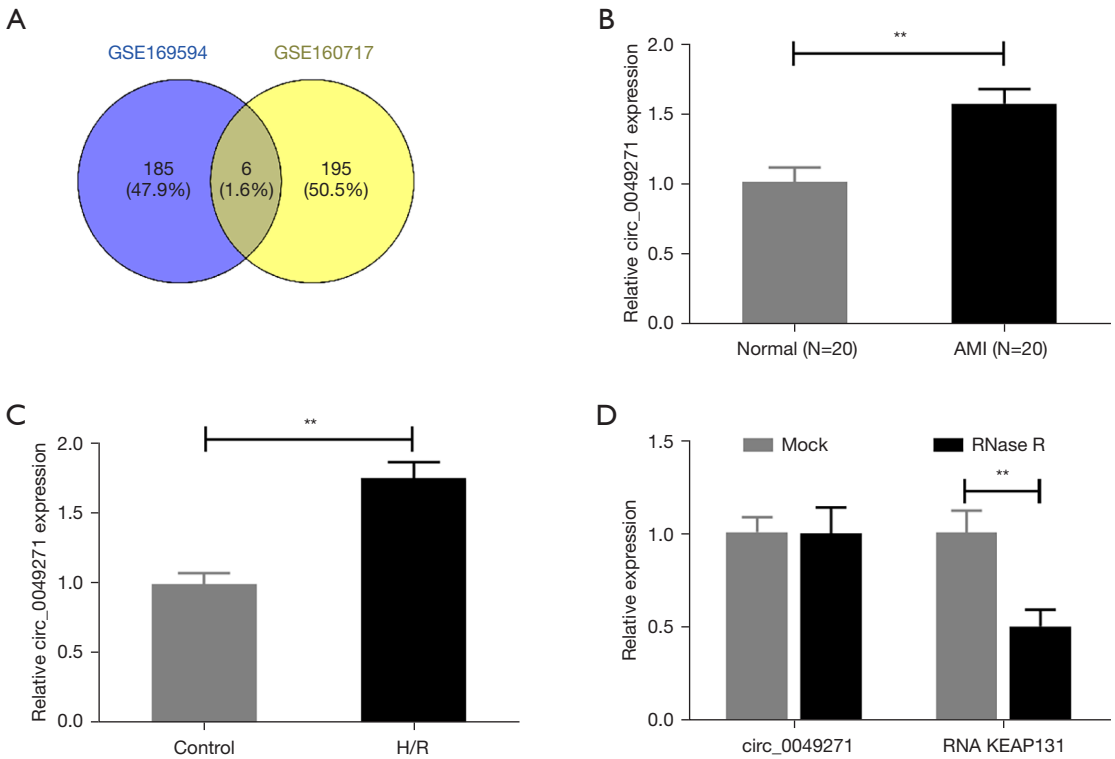

Figure 1 Circ_0049271 was significantly upregulated in the blood and hypoxia-induced H9c2 cells of the AMI patients. (A) A Venn diagram showed the significant upregulation of differential circRNA expression in both the GSE169594 and GSE160717 data sets; (B,C) qRT-PCR was used to detect the circ_0049271 expression in the AMI clinical samples (B) and hypoxia-induced H9c2 cells (C); (D) qRT-PCR was used to determine the circ_0049271 expression level after RNase R treatment, **, P<0.01. H/R, hypoxia-reoxygenation; RNase R, Ribonuclease R; AMI, acute myocardial infarction; qRT-PCR, quantitative reverse transcription-polymerase chain reaction.

Next, qRT-PCR was used to detect circ_0049271 expression in the AMI clinical blood samples and hypoxia-induced H9c2 cells. As a result, the circ_0049271 expression levels in the blood sample of the patients in the AMI group and H9c2 cells in the H/R group were significantly higher than those in the corresponding Normal group and Control group (*Figure 1B,1C*, P<0.01). In addition, the circ_0049271 maintained a stable closed-loop structure after RNase R (Ribonuclease R) treatment (*Figure 1D*), which suggests that circ_0049271 is significantly highly expressed in AMI.

Effects of Circ_0049271 on the proliferation and apoptosis of the H/R-induced H9c2 cells

Circ_0049271 knockdown or overexpression was performed in the H/R-induced myocardial H9c2 cells to explore the function of circ_0049271 in H/R-induced myocardial H9c2 cell injury (*Figure 2A*). Cell proliferation was detected by CCK-8, and apoptosis was detected by flow cytometry and Western Blot. The CCK-8 results showed that the si-circ_0049271 group exhibited a significantly increased proliferation level in the H9c2 cells compared to the si-NC group. However, the proliferation level of cells in the circ_0049271 group was significantly lower than that in the Vector group (*Figure 2B*, P<0.05). Additionally, the flow cytometry results indicated that circ_0049271 knockdown significantly reduced the apoptosis rate of the cells (P<0.05). However, the overexpression of circ_0049271 significantly increased cell apoptosis (P<0.01) (*Figure 2C*,*2D*). The Western blot results showed that the expression level of the pro-apoptotic proteins (i.e., Bax and c-caspase-3) was significantly decreased, and the expression level of the anti-apoptotic Bcl-2 in the cells after si-circ_0049271 knockdown was significantly increased. After circ_004927 overexpression, the protein expression of Bax, c-caspase-3, and Bcl-2 showed the opposite results to those produced by the si-circ_0049271 knockdown (*Figure 2E*). These outcomes suggested that the knockdown of circ_0049271

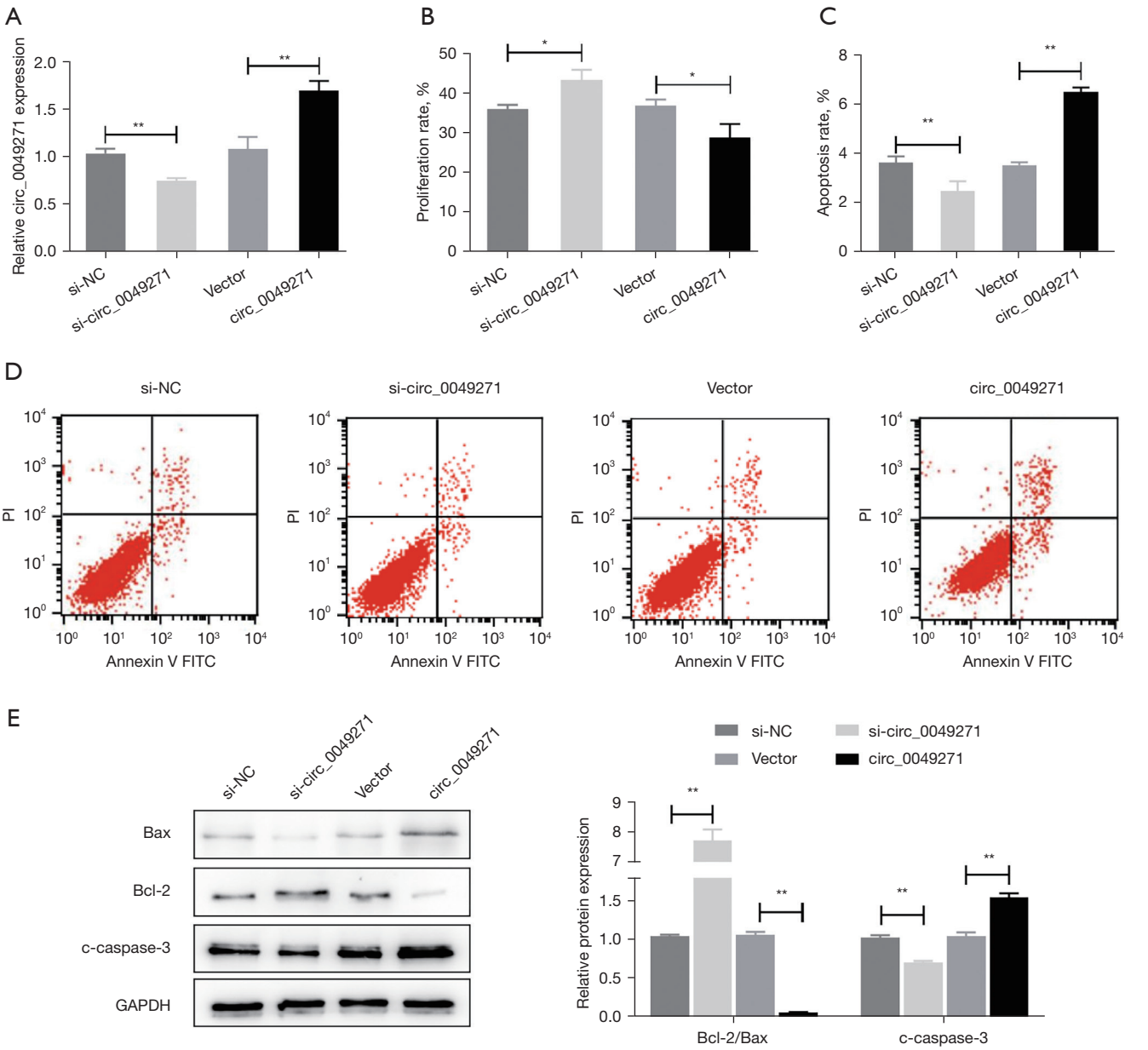

Figure 2 Effects of circ_0049271 on the proliferation and apoptosis of the H9c2 cells with H/R-induced myocardial injury. (A) qRT-PCR was used to detect the circ_0049271 expression level in the cells after the knockdown or overexpression of circ_0049271; (B) CCK-8 was used to detect cell proliferation; (C,D) Flow cytometry was used to detect cell apoptosis; (E) Western blot was used to detect the protein expression of Bax, c-caspase-3, and Bcl-2. *, P<0.05, **, P<0.01. si-NC group, H9c2 cells transfected with the negative control of siRNA. si-circ_0049271 group, H9c2 cells transfected with the circ_0049271 siRNA. Vector group, H9c2 cells transfected with the negative control plasmid. circ_0049271 group, H9c2 cells transfected with the circ_0049271 overexpression plasmid. si-NC, negative control siRNA; PI, isoelectric point; FITC, Fluorescein Isothiocyanate; H/R, hypoxia-reoxygenation; qRT-PCR, quantitative reverse transcription-polymerase chain reaction; CCK-8, Cell Counting Kit-8.

promoted proliferation and inhibited apoptosis in the H/R-induced myocardial injury cells (i.e., the H9c2 cells).

Effects of circ_0049271 on the damage, oxidative stress, and inflammatory response of the H/R-induced H9c2 cells

It was previously reported that the level of myocardial enzymes (CK and LDH) were abnormally increased during myocardial hypoxia-ischemia (26). In this study, we measured the level of related substances to assess whether circ_0049271 could improve H/R-induced injury, oxidative stress, and inflammatory responses in the H9c2 cells. The level of myocardial enzymes (CK and LDH), oxidative stress substances (ROS, MDA, and SOD) and inflammatory factors (IL-1β, IL-6, and IL-8) were determined. The results revealed that after the knockdown of circ_0049271, the activities of LDH and CK and the level of ROS, MDA, IL-1β, IL-6, and IL-8 in the H/R-induced H9c2 cells were significantly decreased, while SOD activity was significantly increased. However, the opposite trend was observed when circ_0049271 was overexpressed in the H/R-induced H9c2 cells; that is, the activities of LDH and CK and the level of ROS, MDA, IL-1β, IL-6, and IL-8 were significantly increased, while SOD activity was significantly decreased (*Figure 3A-3H*, $P<0.05$). Thus, the knockdown of circ_0049271 was shown to significantly alleviate the damage, oxidative stress, and inflammatory response of the H/R-induced H9c2 cells.

Circ_0049271 serves as a sponge for MiR-17-3p

To explore the mechanism of action of circ_0049271, we localized circ_0049271 and found that it was mainly distributed in the cytoplasm (*Figure 4A*). Further, the results of the circbank (http://www.circbank.cn/searchCirc.html) database revealed a relationship between circ_0049271 and miR-17-3p. The luciferase reporter gene experiments confirmed that the co-transfection of the miR-17-3p mimic significantly reduced the luciferase activity of the circ_0049271-WT vector but did not affect the luciferase activity of the circ_0049271-MUT vector (*Figure 4B*). Additionally, the RNA pull-down experiments confirmed the targeting relationship between circ_0049271 and miR-17-3p (*Figure 4C*). Further, in contrast to circ_0049271, the miR-17-3p expression level in the cells of the H/R group was much lower than that in the Control group (*Figure 4D*). The miR-17-3p expression level was significantly increased when circ_0049271 was decreased in the H9c2 cells, while the miR-17-3p level was significantly decreased after circ_0049271 overexpression (*Figure 4E*). Additionally, circ_0049271 was negatively correlated with miR-17-3p expression in the AMI clinical blood samples (*Figure 4F*). Thus, circ_0049271 served as a sponge for miR-17-3p in the cytoplasm of the AMI cells, and miR-17-3p was lowly expressed in AMI.

FZD4 acts as a target of MiR-17-3p

The targeting relationship between miR-17-3p and FZD4 was predicted by the TargetScan database (https://www.targetscan.org/vert_80/) and further examined by dual-luciferase reporter and RNA pull-down experiments (*Figure 5A-5C*). The qRT-PCR results showed that the expression level of FZD4 was significantly higher in the cells of the H/R group than the Control group (*Figure 5D*). Additionally, miR-17-3p in the cells was knocked down or overexpressed by transfection (*Figure 5E*). The transfection results revealed a negative association between the mRNA and protein expression levels of FZD4 and the miR-17-3p level in the cells (*Figure 5F-5H*). FZD4 was also negatively correlated with miR-17-3p in the AMI clinical blood samples (*Figure 5I*). In addition, the FZD4 expression level in the cells was significantly reduced after the knockdown of circ_0049271, while the overexpression of circ_0049271 markedly upregulated the expression level of FZD4 (*Figure 5J*). According to the Pearson correlation analysis, circ_0049271 was positively correlated with FZD4 expression level in the AMI clinical blood samples (*Figure 5K*). These results suggested that FZD4 not only acted as the target gene of miR-17-3p but was also highly expressed in AMI. Further, FZD4 may also function as an oncogene in AMI.

MiR-17-3p knockdown or FZD4 overexpression reverses the effects of si-circ_0049271 on the H/R-induced H9c2 cells

To verify whether circ_0049271 plays a role in AMI through miR-17-3p/FZD4, the H/R-induced H9c2 cells were treated as follows. Circ_0049271 and miR-17-3p were simultaneously knocked down (si-circ_0049271 + miR-17-3p inhibitor group), while circ_0049271 was knocked down, and FZD4 was upregulated (si-circ_0049271 + FZD4 group). The treatment results showed that after the knockdown of circ_0049271, the FZD4 protein expression level was increased by further inhibiting the miR-17-3p

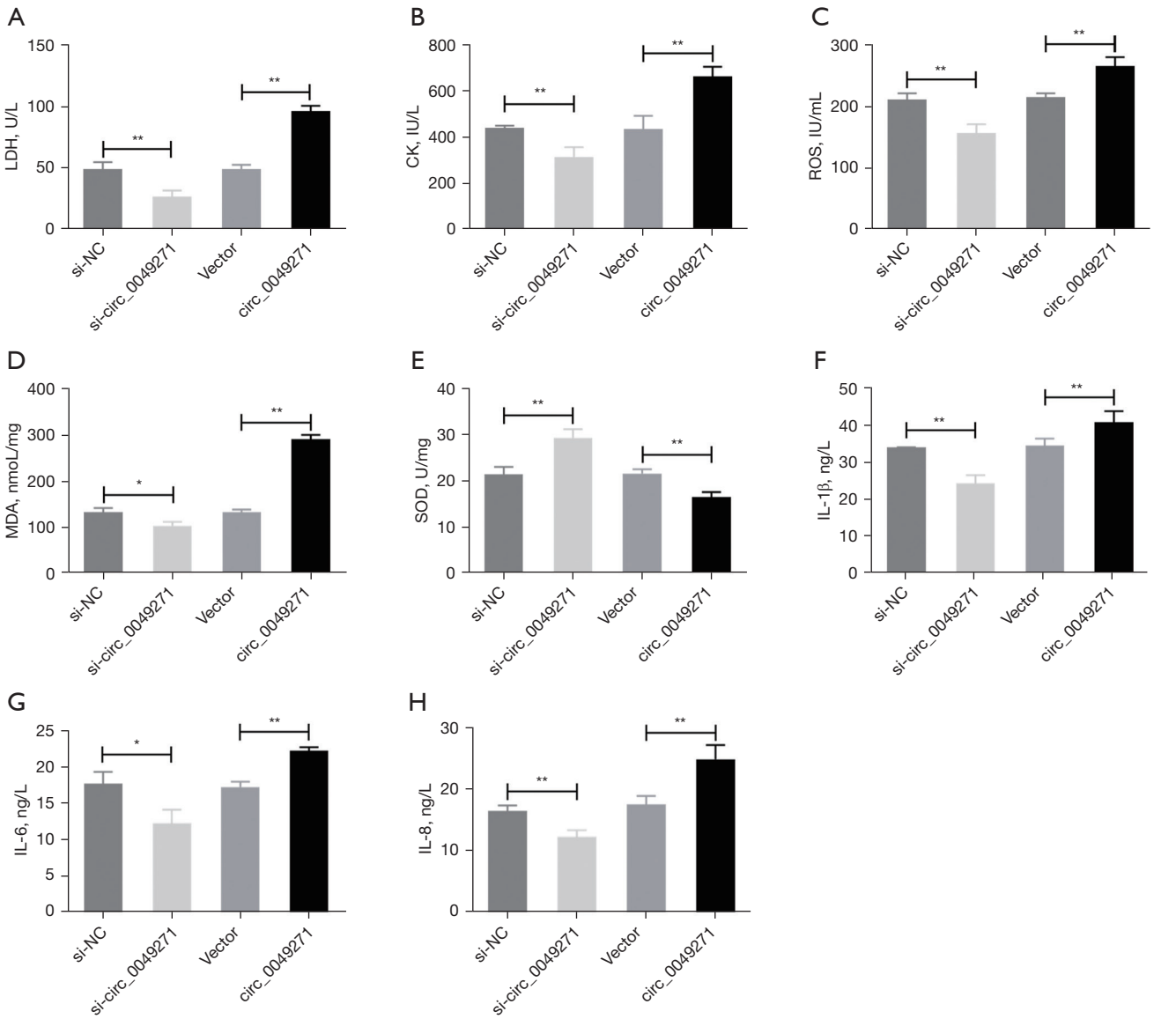

Figure 3 Effects of circ_0049271 on injury, oxidative stress, and inflammatory response in the H/R-induced H9c2 cells. (A-E) A biochemical test was used to determine the level of the myocardial enzymes [LDH (A) and CK (B)] and oxidative stress substances [ROS (C), MDA (D), SOD (E)] in the H/R-induced H9c2 cells after the knockdown or overexpression of circ_0049271; (F-H) ELISA was used to detect the level of inflammatory factors (IL-1β, IL-6, and IL-8) in the H/R-induced H9c2 cells after the knockdown or overexpression of circ_0049271. **, P<0.01; *, P<0.05. LDH, lactate dehydrogenase; si-NC, negative control siRNA; CK, creatine kinase; ROS, reactive oxygen species; MDA, malondialdehyde; SOD, superoxide dismutase; IL, interleukin; H/R, hypoxia-reoxygenation; ELISA, enzyme-linked immunosorbent assay.

expression or overexpression of FZD4 in the H/R-induced H9c2 cells (*Figure 6A,6B*). In sequence, the proliferation, apoptosis, injury, oxidative stress, and inflammatory response of the cells in each group were detected, and the results indicated that the further inhibition of miR-17-3p expression or the overexpression of FZD4 significantly reduced the cell proliferation rate (*Figure 6C*). Additionally, the further inhibition of miR-17-3p expression or the overexpression of FZD4 increased the cell apoptosis rate, promoted the expression of pro-apoptotic-related proteins (c-caspase-3 and Bax), and inhibited the expression of anti-apoptosis-related protein Bcl-2 (*Figure 6D-6G*). Further,

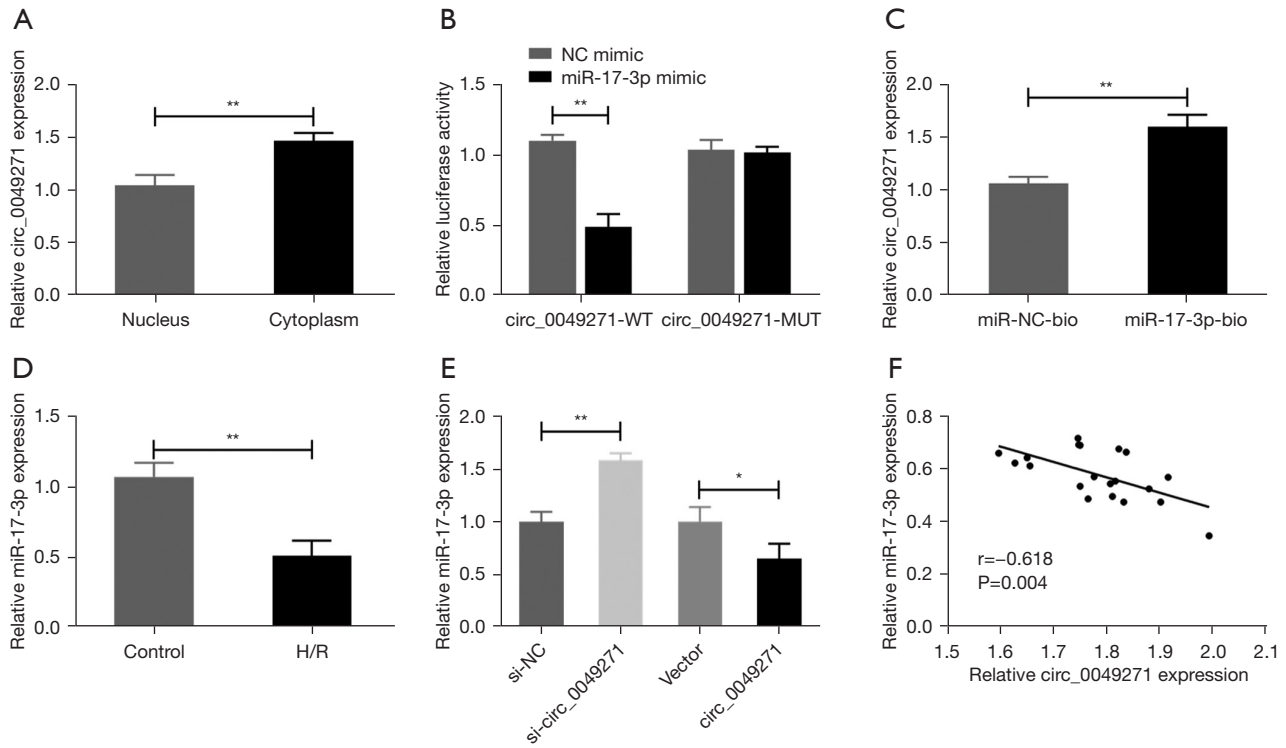

Figure 4 Circ_0049271 served as a sponge for miR-17-3p. (A) qRT-PCR showing circ_0049271 expression levels in the cytoplasm and nucleus. (B) Dual luciferase experiments were used to verify the targeting relationship between circ_0049271 and miR-17-3p, **, P<0.01 *vs.* miR-17-3p group; (C) RNA pull-down experiments were used to verify the targeting relationship between circ_0049271 and miR-17-3p; (D,E) qRT-PCR was used to detect the miR-17-3p expression level in the H/R-induced H9c2 cells of H/R group (D) and the miR-17-3p expression levels in the H9c2 cells after the knockdown or overexpression of circ_0049271 (E); (F) a Pearson correlation analysis was performed to evaluate the correlation between circ_0049271 and miR-17-3p expression in the AMI clinical blood samples. **, P<0.01; *, P<0.05. NC, negative control; WT, wild-type; MUT, mutant; H/R, hypoxia-reoxygenation; si-NC, negative control siRNA; qRT-PCR, quantitative reverse transcription-polymerase chain reaction; AMI, acute myocardial infarction.

H/R-induced H9c2 cell damage, oxidative stress (ROS and MDA) and inflammatory responses were also promoted by some other different treatments, which included increasing the activity of the myocardial enzymes (CK and LDH), and regulating the secretion of the oxidative stress substances and inflammatory factors (*Figure 6H-6O*). To sum up, the knockdown of miR-17-3p or the overexpression of FZD4 reversed the pro-proliferation, anti-apoptosis, anti-oxidative stress, and anti-inflammatory effects of si-circ_0049271 on the H/R-induced H9c2 cells.

Discussion

With the advancement and popularization of high-throughput technology, researchers have discovered that circRNA is a non-coding circular endogenous RNA molecule produced by special alternative splicing (27). CircRNA plays a significant role in various human diseases, including cardiovascular disease (28). It has been reported that some circRNAs [e.g., circ_0060745 (29), circSAMD4A (30), circCDYL (31), and circ_LAS1L (32) affect myocardial cell injury in AMI. At present, the corresponding mechanisms of the above circRNAs have been explored. In our study, the significantly upregulated circRNAs in the AMI-related data sets GSE169594 and GSE160717 were intersected, and 6 common significantly upregulated circRNAs (i.e., hsa_circ_0037516, chr16: 15794592-15794782+, chr3: 16336362-1634509, hsa_circ_0049271, hsa_circ_0076767, and hsa_circ_0023461) were identified. Ren *et al.* found that circ_0023461 expression was upregulated in AMI patients and hypoxia-induced AC16 cells, and the knockdown of circ_0023461 targeted the miR-370-3p/PDE4D axis to

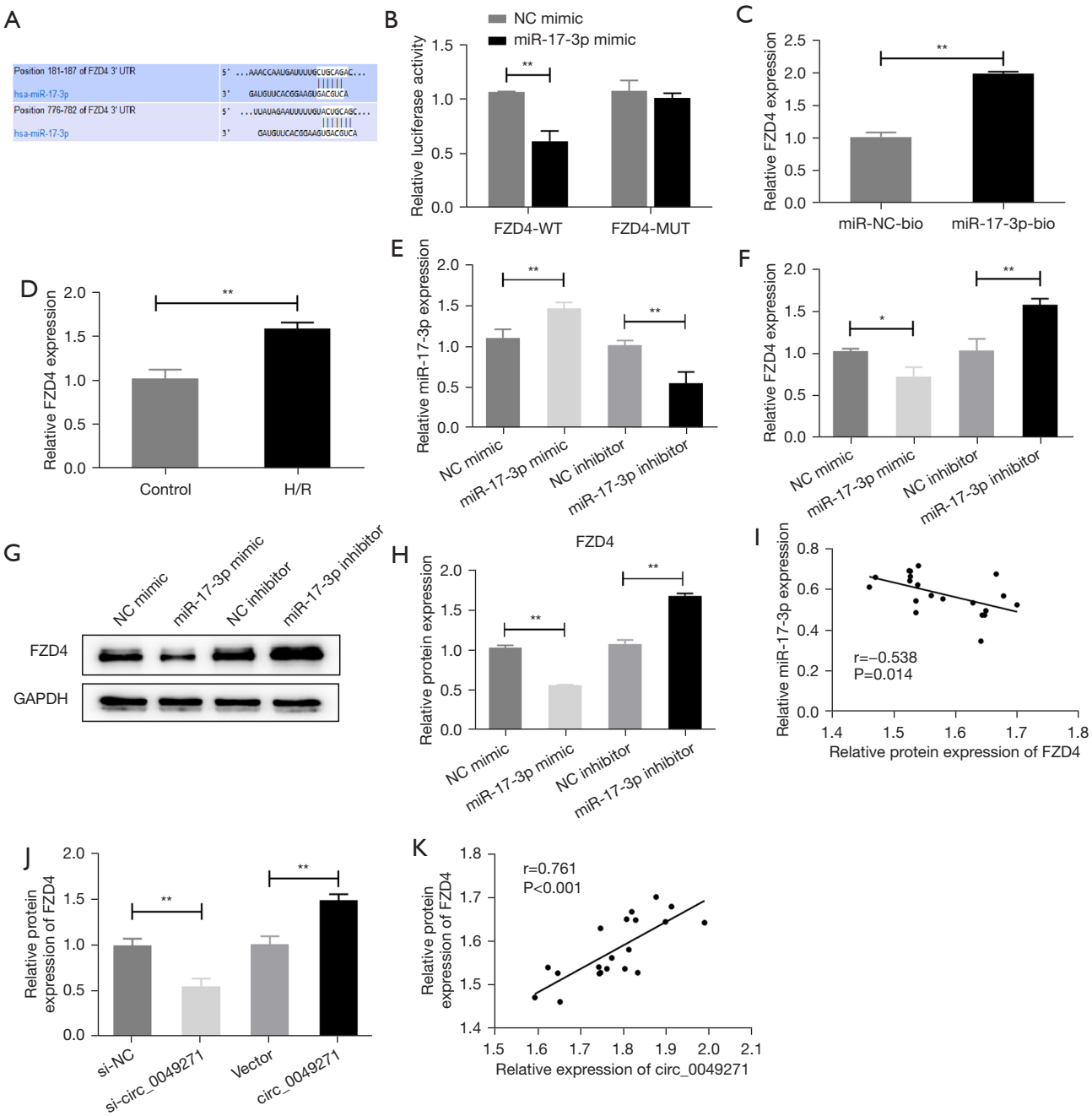

Figure 5 FZD4 acts as the target of miR-17-3p. (A) The targeting sites were predicted by the TargetScan Online website. (B) Dual-luciferase experiments were used to verify the targeting relationship between miR-17-3p and FZD4; (C) RNA pull-down experiments were used to confirm the targeting relationship between miR-17-3p and FZD4; (D-F) qRT-PCR was used to detect the mRNA expression level of FZD4 in the H/R group cells (D), verify the efficiency of the knockdown or overexpression of miR-17-3p in the cells (E), and measure the mRNA expression level of FZD4 after the knockdown or overexpression of miR-17-3p in the cells (F); (G,H) Western blot was used to detect the FZD4 protein expression level after the knockdown or overexpression of miR-17-3p in cells; (I) a Pearson correlation analysis was conducted to analyze the correlation between miR-17-3p and FZD4 expression in the AMI clinical blood samples; (J) qRT-PCR was used to determine the mRNA expression level of FZD4 after the knockdown or overexpression of circ_0049271 in the cells; (K) a Pearson correlation analysis was conducted to analyze the correlation between circ_0049271 and FZD4 expression in the AMI clinical blood samples. **, P<0.01; *, P<0.05. NC, negative control; WT, wild-type; MUT, mutant; si-NC, negative control siRNA; H/R, hypoxia-reoxygenation; qRT-PCR, quantitative reverse transcription-polymerase chain reaction; AMI, acute myocardial infarction.

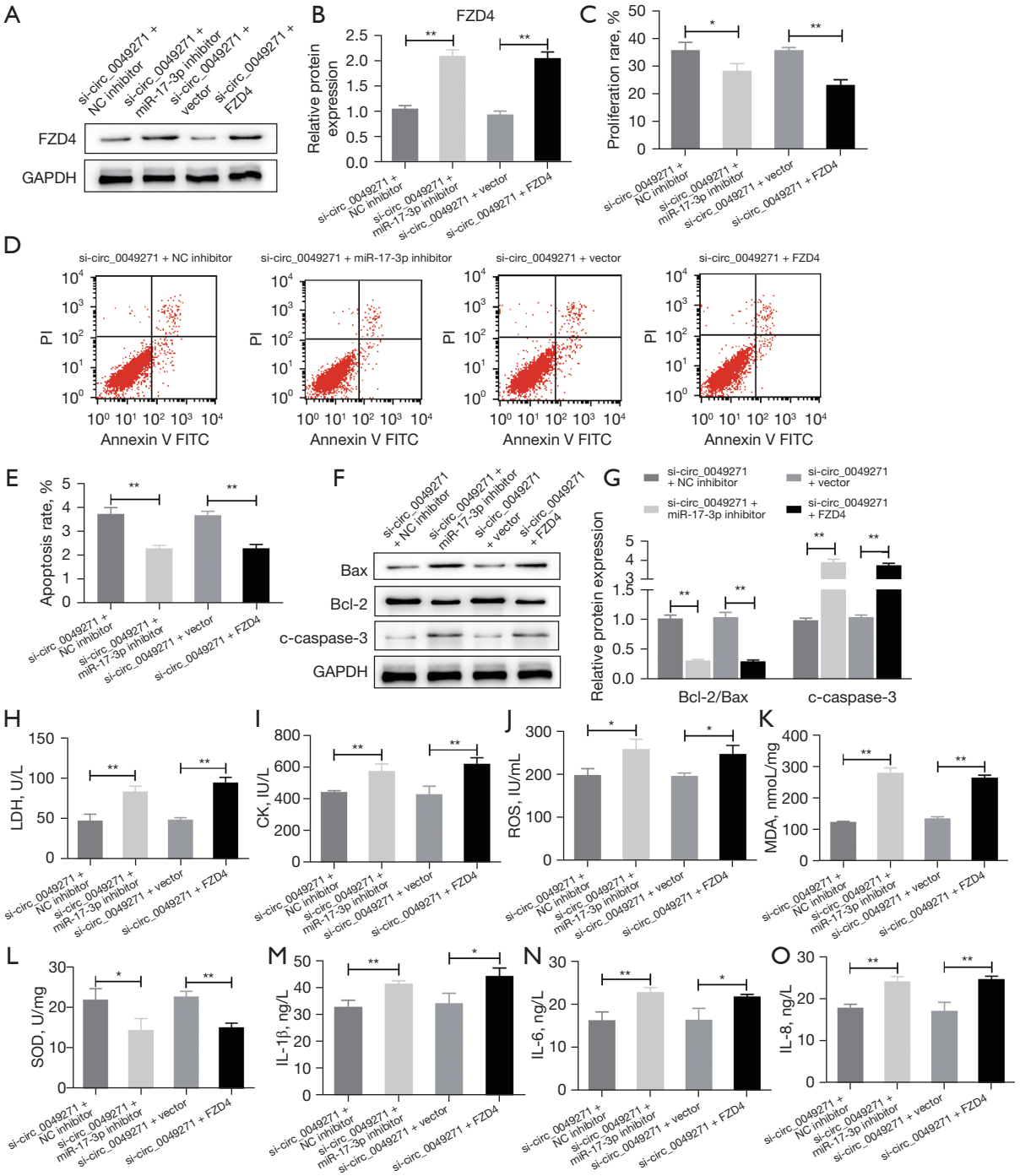

Figure 6 MiR-17-3p knockdown or FZD4 overexpression reversed the effects of si-circ_0049271 on the H/R-induced H9c2 cells. (A,B) Western blot was used to detect the protein expression levels of FZD4 in each group of cells; (C) CCK-8 was used to measure the proliferation rate of each group of cells; (D,E) flow cytometry was used to determine the apoptosis rates of the cells; (F,G) Western blot was used to detect the protein expression levels of the apoptosis-related proteins (i.e., Bax, Bcl-2, and c-caspase-3) in the cells of each group; (H,I) biochemical tests were used to determine the activities of LDH and CK in each group of cells; (J-L) biochemical tests were used to determine the levels of the oxidative stress substances (i.e., ROS, MDA and SOD) in the cells of each group; (M-O) ELISA was used to detect the levels of the inflammatory factors (i.e., IL-1β, IL-6, and IL-8) in the cells of each group. **, P<0.01; *, P<0.05. NC, negative control; PI, isoelectric point; FITC, Fluorescein Isothiocyanate; LDH, lactate dehydrogenase; CK, creatine kinase; ROS, reactive oxygen species; MDA, malondialdehyde; SOD, superoxide dismutase; IL, interleukin; H/R, hypoxia-reoxygenation; ELISA, enzyme-linked immunosorbent assay.

alleviate hypoxia-induced AC16 cell dysfunction (19). However, to date, no studies have examined the functions of the other circRNAs in AMI. In this study, the role and mechanism of circ_0049271 in AMI were explored.

We found that circ_0049271 expression was significantly increased in the blood of the AMI patients and the H/R-induced H9c2 cells. Further, we found that circ_0049271 knockdown alleviated the proliferation inhibition and pro-apoptotic effects of the H/R-induced H9c2 cells, reducing the release of the oxidative stress substances and inflammatory factors, and improving cell damage. However, the overexpression of circ_0049271 produced the opposite effects to that of circ_0049271 knockdown. Given the crucial role of apoptosis and the injury of cardiomyocytes in AMI, it may be that circ_0049271 is involved in the pathogenesis of AMI.

As the target of circRNA, miRNA is the most widely studied non-coding RNA. Specifically, miRNA regulates cell proliferation, differentiation, and apoptosis by degrading target genes or inhibiting the translation (33). Further, miRNAs are involved in cardiac development, cardiac function regulation, cardiac remodeling, and cardiomyocyte apoptosis in the cardiovascular system (34). MiRNAs are also abnormally expressed in cardiovascular diseases (e.g., AMI, angina pectoris, and myocarditis) (35). A study has shown that miRNA-499, miRNA-1, miRNA-133, and miRNA-208 can serve as markers of myocardial injury in AMI (36). MiR-17-92 consists of 6 mature miRNAs (i.e., miR-17, miR-18a, miR-19a, miR-20a, miR-19b1, and miR-92a-1) and is one of the most widely studied miRNA clusters (29). Shi *et al.* showed that miR-17-3p promotes cardiomyocyte hypertrophy, proliferation, and survival and functional recovery after cardiac ischemia/reperfusion (37). Meanwhile, Yuan et al found that inhibition of miR-17-3p aggravated H/R-induced H9c2 injury, and promoted the expression of inflammatory mediators including tumor necrosis factor (TNF)-α, interleukin (IL)-6, IL-1β and phosphorylated NF-κB subunit p65 (38). The present study found that the expression level of miR-17-3p was significantly decreased in in the blood of the AMI patients and H/R-induced H9c2 cells. MiR-17-3p expression was also found to be negatively correlated with circ_0049271 expression. The targeting relationship between circ_0049271 and miR-17-3p was confirmed by dual-luciferase and RNA pull-down experiments. Based on the above outcomes in this study, we speculated that circ_0049271 might function through miR-17-3p.

FZD4, a member of the frizzled gene family, encodes the transmembrane receptor of the Wnt/β-catenin signaling protein (39). Studies have shown that FZD4 is not only abnormally expressed in various cancers (e.g., gastric cancer, breast cancer, non-small cell lung cancer, and liver cancer) but is also associated with the malignant behaviors of these cancers (40,41). In addition, FZD4 is also regulated by circRNA-miRNA. Notably, Zhou *et al.* found that the downregulation of circ_0004712 mediated the miR-331-3p/FZD4 pathway to inhibit the progression of ovarian cancer (42). Zhang *et al.* discovered that circ-ACAP2 promoted colorectal cancer progression by targeting the miR-143-3p/FZD4 axis (43). There are few studies on the function of FZD4 in cardiac injury. A study found that elevated Wnt2 and Wnt4 activate β-catenin/NF-κB signaling to promote cardiac fibrosis by cooperation of FZD4/2 and LRP6 in fibroblasts, which contributes to adverse outcome of patients with AMI (44). In our study, we observed that FZD4 expression was significantly upregulated in the blood of AMI patients and H/R-induced H9c2 cells. Further, FZD4 expression was found to be positively correlated with circ_0049271 and negatively correlated with miR-17-3p. In addition, the targeting relationship between miR-17-3p and FZD4 was further clarified by dual-luciferase and RNA pull-down experiments. FZD4 expression was observed to be significantly upregulated after circ_0049271 and miR-17 were knocked down simultaneously. The functional verification in this study showed that miR-17-3p knockdown or FZD4 overexpression reversed the effects of si-circ_0049271 on the proliferation, apoptosis, oxidative stress, and inflammation of the H/R-induced H9c2 cells. Thus, we conjecture that miR-17-3p/FZD4 is the key molecular mechanism for circ_0049271 affecting H/R-induced H9c2 cell injury.

The present study had some limitations. First, it only explored the function and mechanism of circ_0049271 in the induced AMI model cell-H9c2 cells and did not establish multiple AMI cell models for further verifications. Second, the AMI animal model was not established to verify the function and mechanism of circ_0049271. Thus, further experiments need to be conducted to examine the function and mechanism of circ_0049271.

Conclusions

The expression of circ_0049271 and FZD4 was upregulated

while that of miR-17-3p was significantly downregulated in the blood of the AMI patients and H/R-induced H9c2 cells. In addition, the knockdown of circ_0049271 regulated the miR-17/FZD4 axis to promote cell proliferation, inhibit cell apoptosis and the secretion of oxidative stress substances and inflammatory factors, and improve the damage of the H/R-Induced H9c2 cells. Taken together, our results suggest that circ_0049271 could serve as a potential therapeutic target for AMI.

Acknowledgments

Funding: None.

Footnote

Reporting Checklist: The authors have completed the MDAR reporting checklist. Available at https://atm.amegroups.com/article/view/10.21037/atm-22-6331/rc

Data Sharing Statement: Available at https://atm.amegroups.com/article/view/10.21037/atm-22-6331/dss

Conflicts of Interest: All authors have completed the ICMJE uniform disclosure form (available at https://atm.amegroups.com/article/view/10.21037/atm-22-6331/coif). The authors have no conflicts of interest to declare.

Ethical Statement: The authors are accountable for all aspects of the work in ensuring that questions related to the accuracy or integrity of any part of the work are appropriately investigated and resolved. The study was conducted in accordance with the Declaration of Helsinki (as revised in 2013). The study was approved by the Research Ethics Committee of Huizhou Third People's Hospital (No. 2022-8) and informed consent was taken from all the participants.

References

1. Gulati R, Behfar A, Narula J, et al. Acute Myocardial Infarction in Young Individuals. Mayo Clin Proc 2020;95:136-56.
2. Shibata T, Kawakami S, Noguchi T, et al. Prevalence, Clinical Features, and Prognosis of Acute Myocardial Infarction Attributable to Coronary Artery Embolism. Circulation 2015;132:241-50.
3. Amsterdam EA, Wenger NK, Brindis RG, et al. 2014 AHA/ACC Guideline for the Management of Patients with Non-ST-Elevation Acute Coronary Syndromes: a report of the American College of Cardiology/American Heart Association Task Force on Practice Guidelines. J Am Coll Cardiol 2014;64:e139-e228.
4. Caballero EP, Santamaria MH, Corral RS. Endogenous osteopontin induces myocardial CCL5 and MMP-2 activation that contributes to inflammation and cardiac remodeling in a mouse model of chronic Chagas heart disease. Biochim Biophys Acta Mol Basis Dis 2018;1864:11-23.
5. Gan W, Ren J, Li T, et al. The SGK1 inhibitor EMD638683, prevents Angiotensin II-induced cardiac inflammation and fibrosis by blocking NLRP3 inflammasome activation. Biochim Biophys Acta Mol Basis Dis 2018;1864:1-10.
6. Panda AC. Circular RNAs Act as miRNA Sponges. Adv Exp Med Biol 2018;1087:67-79.
7. Yang Y, Yujiao W, Fang W, et al. The roles of miRNA, lncRNA and circRNA in the development of osteoporosis. Biol Res 2020;53:40.
8. Altesha MA, Ni T, Khan A, et al. Circular RNA in cardiovascular disease. J Cell Physiol 2019;234:5588-600.
9. Akhter R. Circular RNA and Alzheimer's Disease. Adv Exp Med Biol 2018;1087:239-43.
10. Zhang Z, Yang T, Xiao J. Circular RNAs: Promising Biomarkers for Human Diseases. EBioMedicine 2018;34:267-74.
11. Zhang HD, Jiang LH, Sun DW, et al. CircRNA: a novel type of biomarker for cancer. Breast Cancer 2018;25:1-7.
12. Zhou LY, Zhai M, Huang Y, et al. The circular RNA ACR attenuates myocardial ischemia/reperfusion injury by suppressing autophagy via modulation of the Pink1/FAM65B pathway. Cell Death Differ 2019;26:1299-315.
13. Li Y, Ren S, Xia J, et al. EIF4A3-Induced circ-BNIP3 Aggravated Hypoxia-Induced Injury of H9c2 Cells by Targeting miR-27a-3p/BNIP3. Mol Ther Nucleic Acids

2020;19:533-45.
14. Miao L, Yin RX, Zhang QH, et al. A novel circRNA-miRNA-mRNA network identifies circ-YOD1 as a biomarker for coronary artery disease. Sci Rep 2019;9:18314.
15. Xing X, Guo S, Zhang G, et al. miR-26a-5p protects against myocardial ischemia/reperfusion injury by regulating the PTEN/PI3K/AKT signaling pathway. Braz J Med Biol Res 2020;53:e9106.
16. Li B, Wang Z, Yu M, et al. miR-22-3p enhances the intrinsic regenerative abilities of primary sensory neurons via the CBL/p-EGFR/p-STAT3/GAP43/p-GAP43 axis. J Cell Physiol 2020;235:4605-17.
17. Yuan J, Chen H, Ge D, et al. Mir-21 Promotes Cardiac Fibrosis After Myocardial Infarction Via Targeting Smad7. Cell Physiol Biochem 2017;42:2207-19.
18. Lu D, Tang L, Zhuang Y, et al. miR-17-3P regulates the proliferation and survival of colon cancer cells by targeting Par4. Mol Med Rep 2018;17:618-23.
19. Ren K, Li B, Jiang L, et al. circ_0023461 Silencing Protects Cardiomyocytes from Hypoxia-Induced Dysfunction through Targeting miR-370-3p/PDE4D Signaling. Oxid Med Cell Longev 2021;2021:8379962.
20. Li Y, Shi R, Zhu G, et al. Construction of a circular RNA-microRNA-messenger RNA regulatory network of hsa_circ_0043256 in lung cancer by integrated analysis. Thorac Cancer 2022;13:61-75.
21. Li L, Sun D, Li X, et al. Identification of Key circRNAs in Non-Small Cell Lung Cancer. Am J Med Sci 2021;361:98-105.
22. Zhang J, Liu Y, Shi G. The circRNA-miRNA-mRNA regulatory network in systemic lupus erythematosus. Clin Rheumatol 2021;40:331-9.
23. Zeng L, Zhang P, Fang Z, et al. The Construction and Analysis of Infiltrating Immune Cell and ceRNA Networks in Diabetic Foot Ulcer. Front Endocrinol (Lausanne) 2022;13:836152.
24. Du J, Zhang L, Zhuang S, et al. HDAC4 degradation mediates HDAC inhibition-induced protective effects against hypoxia/reoxygenation injury. J Cell Physiol 2015;230:1321-31.
25. Oliveros JC. Venny. An interactive tool for comparing lists with Venn's diagrams. 2007-2015.
26. Aggarwal S, Randhawa PK, Singh N, et al. Role of ATP-Sensitive Potassium Channels in Remote Ischemic Preconditioning Induced Tissue Protection. J Cardiovasc Pharmacol Ther 2017;22:467-75.
27. Yin L, Tang Y, Jiang M. Research on the circular RNA bioinformatics in patients with acute myocardial infarction. J Clin Lab Anal 2021;35:e23621.
28. Guo Y, Luo F, Liu Q, et al. Regulatory non-coding RNAs in acute myocardial infarction. J Cell Mol Med 2017;21:1013-23.
29. Zhai C, Qian G, Wu H, et al. Knockdown of circ_0060745 alleviates acute myocardial infarction by suppressing NF-kappaB activation. J Cell Mol Med 2020;24:12401-10.
30. Hu X, Ma R, Cao J, et al. CircSAMD4A aggravates H/R-induced cardiomyocyte apoptosis and inflammatory response by sponging miR-138-5p. J Cell Mol Med 2022;26:1776-84.
31. Wang J, Cai H, Liu Q, et al. Cinobufacini Inhibits Colon Cancer Invasion and Metastasis via Suppressing Wnt/β-Catenin Signaling Pathway and EMT. Am J Chin Med 2020;48:703-18.
32. Sun LY, Zhao JC, Ge XM, et al. Circ_LAS1L regulates cardiac fibroblast activation, growth, and migration through miR-125b/SFRP5 pathway. Cell Biochem Funct 2020;38:443-50.
33. Wang Q, Liu B, Wang Y, et al. The biomarkers of key miRNAs and target genes associated with acute myocardial infarction. PeerJ 2020;8:e9129.
34. Navickas R, Gal D, Laucevicius A, et al. Identifying circulating microRNAs as biomarkers of cardiovascular disease: a systematic review. Cardiovasc Res 2016;111:322-37.
35. Cheng M, Yang J, Zhao X, et al. Circulating myocardial microRNAs from infarcted hearts are carried in exosomes and mobilise bone marrow progenitor cells. Nat Commun 2019;10:959.
36. Fan PC, Chen CC, Peng CC, et al. A circulating miRNA signature for early diagnosis of acute kidney injury following acute myocardial infarction. J Transl Med 2019;17:139.
37. Shi J, Bei Y, Kong X, et al. miR-17-3p Contributes to Exercise-Induced Cardiac Growth and Protects against Myocardial Ischemia-Reperfusion Injury. Theranostics 2017;7:664-76.
38. Yuan T, Yang Z, Xian S, et al. Dexmedetomidine-mediated regulation of miR-17-3p in H9C2 cells after hypoxia/reoxygenation injury. Exp Ther Med 2020;20:917-25.
39. Poulter JA, Ali M, Gilmour DF, et al. Mutations in TSPAN12 Cause Autosomal-Dominant Familial Exudative Vitreoretinopathy. Am J Hum Genet 2016;98:592.
40. Yang Y, Sun Y, Wu Y, et al. Downregulation of miR-3127-5p promotes epithelial-mesenchymal transition via FZD4 regulation of Wnt/beta-catenin signaling in non-small-cell

lung cancer. Mol Carcinog 2018;57:842-53.
41. Strakova K, Matricon P, Yokota C, et al. The tyrosine Y250(2.39) in Frizzled 4 defines a conserved motif important for structural integrity of the receptor and recruitment of Disheveled. Cell Signal 2017;38:85-96.
42. Zhou X, Jiang J, Guo S. Hsa_circ_0004712 downregulation attenuates ovarian cancer malignant development by targeting the miR-331-3p/FZD4 pathway. J Ovarian Res 2021;14:118.
43. Zhang G, Liu Z, Zhong J, et al. Circ-ACAP2 facilitates the progression of colorectal cancer through mediating miR-143-3p/FZD4 axis. Eur J Clin Invest 2021;51:e13607.
44. Yin C, Ye Z, Wu J, et al. Elevated Wnt2 and Wnt4 activate NF-kappaB signaling to promote cardiac fibrosis by cooperation of Fzd4/2 and LRP6 following myocardial infarction. EBioMedicine 2021;74:103745.

(English Language Editor: L. Huleatt)

Cite this article as: Liao H, Xiao C, Li W, Chen W, Xiang D. Silencing hsa_circ_0049271 attenuates hypoxia-reoxygenation (H/R)-induced myocardial cell injury via the miR-17-3p/FZD4 signaling axis. Ann Transl Med 2023;11(2):99. doi: 10.21037/atm-22-6331